

Ultratrace analysis of Antarctic snow samples by reaction cell inductively coupled plasma mass spectrometry using a total-consumption micro-sample-introduction system

Marco Grotti,^{*a} Francesco Soggia^a and José Luis Todoli^b

Received 10th March 2008, Accepted 11th June 2008

First published as an Advance Article on the web 28th July 2008

DOI: 10.1039/b804043e

In this work, a new sensitive procedure for the determination of ultratrace elements in snow samples based on quadrupole ICP-MS has been developed. After filtration through a 0.5 μm PTFE membrane (for dissolved element determination) or acidification with 0.5% nitric acid (for acid dissolvable element determination), the analytes were preconcentrated by sample volume reduction and analysed by ICP-MS. Micro-samples were efficiently introduced into the plasma source at 20 $\mu\text{l min}^{-1}$ uptake rate by using a PFA micronebulizer coupled to an evaporation chamber of the torch integrated sample introduction system (TISIS). As a result, the amount of sample required was about one order of magnitude lower than that required with a conventional liquid sample introduction system. In order to improve the transport efficiency, the TISIS chamber was electrically-heated at 70 $^{\circ}\text{C}$ and a sheathing gas stream was used to protect the aerosol from the chamber walls. Under these conditions, negative solvent plasma effects were no more severe than for conventional systems, because the total solvent plasma load was 20 mg min^{-1} . The operating parameters were optimized to obtain maximum sensitivity, while limiting oxides and double charge ion formation. The polyatomic interferences were removed by applying the dynamic reaction cell (DRC) technique, using ammonia as the reaction gas. Under the optimized conditions, limits of detection ranged from 0.02 to 4.5 pg g^{-1} , allowing the determination of Cr, V, Fe, Mn, Pb, Zn, Cd, Co and Cu in Antarctic snow samples. Signal repeatability was lower than 10% which prevented the use of an internal standard. Precision of the procedure ranged from 2.0% to 5.6%. The accuracy of the method was verified by the analysis of both certified reference water and surface snow samples collected in coastal and inland areas of Antarctica. The DRC program used, the short wash out and signal stabilization times registered under these conditions led to a 10 h^{-1} sample throughput.

Introduction

The determination of heavy metals in Antarctic and Greenland snow and ice caps is of great interest as it provides valuable information on past and recent changes in the chemical composition of earth's atmosphere.^{1,2} Further, the analysis of surface snow permits the evaluation of the current quality of the polar environments,^{3,4} to assess the impact of human activity⁵ and to investigate the sources and transport pathways of contaminants.^{6,7}

Heavy metal concentrations in polar ice and snow samples is extremely low, typically at or below the pg g^{-1} level. Hence, in order to obtain reliable data, the application of "ultraclean" procedures for sampling, storage, treatment and analysis, as well as the achievement of very high instrumental sensitivity are necessary.⁸ For heavy metals determination in polar snow samples, several analytical techniques have been used,

including graphite furnace atomic absorption spectrometry,⁹⁻¹¹ laser excited atomic fluorescence spectrometry,¹²⁻¹⁴ differential pulse anodic stripping voltammetry,^{15,16} instrumental neutron activation analysis¹⁷ and inductively coupled plasma mass spectrometry (ICP-MS).^{3,8,18-22} Jickells and co-workers¹⁸ reported the determination of trace elements in snowfall of the remote Scottish Highlands at the ng g^{-1} level by using quadrupole ICP-MS. The samples were filtered on a 0.45 μm membrane to provide dissolved/particulate distributions and a 7-fold preconcentration step by non-boiling evaporation was applied before the ICP-MS analysis of the dissolved phase. Sturgeon and co-workers¹⁹ reported the direct determination of ultratrace levels of heavy metals in arctic snow by electrothermal vaporization ICP-MS. In recent years, the high resolution ICP-MS has emerged as the analytical technique of choice for ultrasensitive determination of heavy metals at the sub-picogram per gram level, as it provides superior performances in terms of detection power, multi-element capability and low sample consumption.^{3,8,20,21} For example, detection limits ranging from 0.09 to 0.9 pg g^{-1} have been achieved by Barbante *et al.*,²⁰ allowing direct and simultaneous determination of Co, Cu, Zn, Mo, Pd, Ag, Cd, Sb, Pt, Pb, Bi and U in Greenland and Antarctic

^aDipartimento di Chimica e Chimica Industriale - Università di Genova, Via Dodecaneso 31, 16146, Genoa, Italy. E-mail: grotti@chimica.unige.it

^bDepartamento de Química Analítica, Nutrición y Bromatología - Universidad de Alicante, 03080, Alicante, España

snow samples, with adequate repeatability (8–25% depending on the element). A further improvement in sensitivity for the analysis of snow samples by high resolution ICP-MS has been obtained using ultrasonic nebulization.²² On the other hand, the technique is quite expensive, it requires well-trained operators and its sensitivity drastically decreases when the high resolution mode has to be applied to resolve spectral interferences.²³

So far, snow analysis through double focusing ICP-MS has been performed with conventional liquid sample introduction systems operated at liquid flow rates on the order of 1 ml min⁻¹.²⁰ With this method, the sample mass required to carry out the analysis is rather high. In order to further reduce the amount of sample required, a micronebulizer has been coupled to a double pass spray chamber.^{3,24} In this case, the system has been operated at delivery flow rates of up to 80 µl min⁻¹ and the sample volume required to perform the analysis is close to 1 ml. The volume of sample required was the result of three main reasons: the somewhat high liquid flow rates,²⁰ the long spray chamber wash out times and, for the lowest concentrations, the requirement for a sample pre-concentration step.³ Other features of the reported methods are the moderate signal stabilization times (*i.e.*, 40 s–1 min) and repeatability of the measurements ranging between 9% and 34%.

The aim of this study was the development of a new analytical method for trace element determination in snow samples using quadrupole ICP-MS with a minimum sample consumption. In order to achieve this result, the investigation was focused on three aspects, namely: (i) the development of a simple and clean pre-concentration procedure by sample volume reduction; (ii) the application of a new total-consumption micro-sample-introduction system based on the so-called torch integrated sample introduction system (TISIS);^{25,26} and (iii) the optimization of the ICP-MS analysis using the dynamic reaction cell technique^{27–29} to minimize the polyatomic interferences. The optimized procedure was applied to the analysis of both certified reference material and surface snow samples collected in coastal and inland areas of Antarctica.

Experimental

Chemicals

Ultrapure water was supplied by the four column ion-exchange system Milli-Q, fed by the reverse osmosis system Elix 3, both from Millipore (El Paso, TX, USA). Analytical-grade 65% nitric acid from Carlo Erba (Milano, Italy) and suprapur[®] 65% nitric acid from Merck (Darmstadt, Germany) were used for the cleaning of materials. Trace Select[®] Ultra 65% nitric acid from Sigma–Aldrich (St. Louis, MO, USA) was used for the final stage of the cleaning procedure of materials (see below) and for the preparation of standards and samples.

1000 mg l⁻¹ single-element standard solutions were obtained from Sigma–Aldrich. Daily standards were prepared by serial dilution with 0.05% (v/v) nitric acid solution. Standard solutions for daily-performance check and tuning were supplied by PerkinElmer-Sciex (Concord, Ontario, Canada). Ammonia (99.9995%) was purchased from SIAD (Bergamo, Italy) and used as the reaction gas.

Materials

Wide-mouthed 1 litre and 2 litre LDPE bottles were purchased from Nalgene (Rochester, NY, USA) and used for surface snow collection and storage. 15 ml and 50 ml PP graduated conical test tubes with tight screw caps were supplied by Kartel (Milan, Italy) and used for the preparation of standards and samples. All these materials were extensively acid-cleaned following a five-step procedure: (1) 10% (v/v) analytical-grade nitric acid for 1 week and rinsing with ultrapure water; (2) 1% (v/v) suprapur[®] nitric acid for 2–3 days and rinsing with ultrapure water; (3–4) repetitions of step 2; (5) 0.1% (v/v) Trace Select[®] Ultra nitric acid until use and rinsing with ultrapure water just before use.

Samples

Surface snow samples were collected at three Antarctic sites: (a) Terra Nova Bay (74°43'N; 164°07'E); (b) Talos Dome (72°50'S 159°12'E; elevation: 2300 m; 275 km from the coast) and Dome C (75°07'N; 123°19'E; elevation: 3200 m; 1200 km from the coast), during the Italian Antarctic expeditions from 2001 to 2006. In order to prevent contamination during sampling, operators wore clean room clothes and approached the sampling site upwind. The samples were collected in pre-cleaned LDPE bottles, sealed inside double polyethylene bags and stored at –30 °C until analysis in the Antarctic Environmental Specimen Bank.³⁰ The certified reference water TM-23.3 was supplied by the Environment Canada's NWRI (<http://www.nwri.ca/about-e.html>) and used for method validation.

Sample preparation

(a) *Dissolved element determination.* Under a laminar flow hood, samples were allowed to melt and filtered through 0.5 µm PTFE membrane filter (FHLC02500, Millipore). After, 10 ml aliquots were transferred into acid-cleaned 15 ml graduated vessels and refrozen until analysis. Then, the samples were freeze-dried, re-dissolved in 200 µl of 0.05% ultrapur-grade nitric acid solution and analysed by ICP-MS.

(b) *Acid dissolvable element determination.* Samples were allowed to melt under a laminar flow hood, after which 10 ml aliquots were transferred into acid-cleaned 15 ml graduated vessels, acidified with 50 µl of ultrapur-grade nitric acid and refrozen until analysis. Then, the samples were freeze-dried, re-dissolved in 200 µl of 0.05% ultrapur-grade nitric acid solution and analysed by ICP-MS. For each procedure, ten procedural blanks were run in order to evaluate any contamination artifacts.

Sample analysis

The ICP-MS system used was a PerkinElmer-Sciex (Concord, Ontario, Canada) Elan DRC II. Instrumental characteristics and operating parameters are listed in Tables 1–2. The sample introduction system was adapted from the so-called torch integrated sample introduction system (TISIS),^{25,26} especially designed for the analysis of liquid microsamples in ICP spectrometry. It consists of a single-pass evaporation chamber, with a lateral port to introduce a sheathing gas stream, in a location close to the aerosol production point. A Teflon adapter is used to fit the micronebulizer to the chamber base and the cavity is directly jointed with the quartz injector of the plasma torch.

Table 1 Instrumental characteristics and operating parameters

Instrument	PerkinElmer-Sciex Elan DRC II
Sample introduction system	TISIS ^{25,26}
Nebulizer	PFA-ST microconcentric
Spray chamber	Single pass, heated at 70 °C
Nebulizer gas flow rate	0.8 l min ⁻¹
Sheathing gas flow rate	0.1 l min ⁻¹
Sample uptake rate	20 µl min ⁻¹
Injector	Quartz (2.0 mm id)
Plasma source	Free-running (nominal 40 MHz) ICP
RF power	1400 W
Plasma gas flow rate	14.5 l min ⁻¹
Auxiliary gas flow rate	1.65 l min ⁻¹
Interface	
Sampler	1.1 mm diameter Pt
Skimmer	0.9 mm diameter Pt
Ion optics	Grounded metal stop disk + single cylinder lens, voltage ramped with mass (Autolens [®])
Lens voltage at $m/z = 24$	6.4 V
Lens voltage at $m/z = 115$	8.6 V
Lens voltage at $m/z = 208$	11.2 V
Reaction cell	Dynamic Reaction cell (DRC)
RF amplitude	150 V
Axial field voltage	300 V
Cell path voltage	-28 V
Rod offset	-1 V
Reaction gas	NH ₃
Gas flow rate	See Table 2
Stability parameters	See Table 2
Mass analyser	Quadrupole
Rod offset	-8 V
Detector	Dual analog/digital discrete dynode
Analog stage voltage	-2350 V
Pulse stage voltage	1150 V
Signal measurement	
Acquisition mode	Peak-hopping
Dwell time	50 ms (100 ms for Fe)
Sweeps	20
Replicates	10

The chamber was electrically-heated at 70 °C by means of a wounded heating tape connected to a DC power supply (12 V; 0.3 A). A Glass Expansion (Melbourne, Australia) Cinnabar spray chamber with a 20 ml inner volume was taken as the reference system.

The RF power, the nebulizer gas flow rate and the sheathing gas flow rate were optimized to obtain maximum sensitivity, while limiting oxides and double charge ion formation (¹⁵⁶CeO⁺/¹⁴⁰Ce⁺ < 0.02; ¹³⁸Ba²⁺/¹³⁸Ba⁺ < 0.03). The voltage of the cylinder lens, the rod offset voltages of both the quadrupole and the reaction cell as well as the Mathieu stability parameters

Table 2 ICP-MS analytical program

Analyte	Mode	Reactive gas flow rate ^a	Stability parameters ^b	
			RPa	RPq
Fe	DRC	1.0	0.0	0.6
Cr	DRC	0.4	0.0	0.6
V	DRC	0.4	0.0	0.6
Mn	DRC	0.4	0.0	0.6
Pb	Standard	0.0	0.0	0.25
Zn	Standard	0.0	0.0	0.25
Cd	Standard	0.0	0.0	0.25
Co	Standard	0.0	0.0	0.25
Cu	Standard	0.0	0.0	0.25

^a Values in Ar-equivalent cm³ min⁻¹. ^b Mathieu stability parameters of the cell's quadrupole: $a = 1.9*RPa$; $q = 0.95*RPq$.

a and q of the cell's quadrupole were optimized for maximum ion transmission. The RF amplitude of the DRC, the axial field voltage and the cell path voltage were set according to Tanner *et al.*²⁹ The signal measurement parameters were optimized in order to achieve the best instrumental precision, while consuming less than 200 µl of sample.

Results and discussion

Optimization of the micro-sample-introduction system

In order to analyse sub-millilitre samples coming from the pre-concentration procedure, the use of a suitable micro-sample-introduction system was required. Recent investigations^{25,26} showed that the torch integrated sample introduction system (TISIS), especially designed for the analysis of liquid microsamples in plasma source atomic spectrometry, provides superior performances over the conventional devices. The main advantages include: (i) higher sensitivities, (ii) lower limits of detection, (iii) less intense non spectroscopic interferences, (iv) shorter wash out times and (v) lower memory effects. Hence, we decided to apply this system for the ICP-MS analysis of the preconcentrates. In order to improve the transport efficiency, the TISIS chamber was electrically-heated at 70 °C and a sheathing gas stream was used to protect the aerosol from the chamber walls. Contrarily, previous studies dealing with snow samples have highlighted the benefits of working with a cooled spray chamber system.^{3,20,24} However, cooling the spray chamber to prevent the solvent transport towards the plasma leads to a drop in the mass of analyte delivered to it and, hence, in the sensitivity thus leading to worse ICP-MS LODs.³¹

Heating the spray chamber walls can be detrimental from the point of view of plasma stability. However, in order to mitigate the negative effects of the solvent plasma load low liquid flow rates can be used. The mass of water that can be accepted by an ICP operated at a RF power value on the order of 1–1.5 kW is included within the 20–40 mg min⁻¹ range. Assuming a 100% solvent transport efficiency, the solvent plasma load at the liquid flow rate selected in the present study would be 20 mg min⁻¹. Another problem of heating the spray chamber is related with the sudden evaporation of the droplets as they impact against the hot chamber walls. This causes degradation of the signal's short term stability.³² Furthermore, signal spikes

can be found as dry analyte particles can be renebulized from the chamber walls or nebulizer tip.³³ In the present work, these unwanted effects were solved by employing an argon stream that acted as a shield, thus avoiding the droplet impact against the cavity walls. The achieved short term stability for two representative ions ($^{115}\text{In}^+$ and $^{208}\text{Pb}^+$) and the oxides formation (quantified by the $^{156}\text{CeO}^+ / ^{140}\text{Ce}^+$ ion intensity ratio) was very good. As it can be observed from Fig. 1, the RSD of the signal measurements taken for about 15 min was always lower than 4%. As a consequence accurate and precise sample analysis was possible without applying internal standardization.

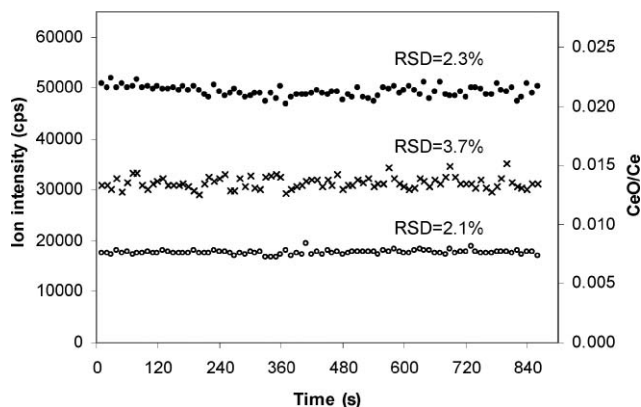


Fig. 1 Short term stability of the signals corresponding to $^{115}\text{In}^+$ (●) and $^{208}\text{Pb}^+$ (○) ions and of the $^{156}\text{CeO}^+ / ^{140}\text{Ce}^+$ ratio (×). Analytical concentration: $1 \mu\text{g l}^{-1}$; integration time: 2000 ms.

The effect of the sheathing gas flow rate on the ion intensity at three representative m/z values (corresponding to $^{24}\text{Mg}^+$, $^{115}\text{In}^+$ and $^{208}\text{Pb}^+$ ions) and on the oxide formation are shown in Fig. 2. It can be seen that both the ion signals and the oxides formation significantly increased with increasing the sheathing gas flow rate, due to the improved aerosol transport towards the plasma source. Besides, provided that the total central gas flow rate increased, the plasma ion production zone was degraded which also favoured the production of oxides. This latter factor can be verified by comparing the ion intensity enhancement factor for the analytes (mainly due to transport improvement) and that for CeO/Ce (related with both solvent transport and plasma degradation) when switching from no sheathing gas to 0.2 l min^{-1} sheathing gas flow rate. Thus for In the signal

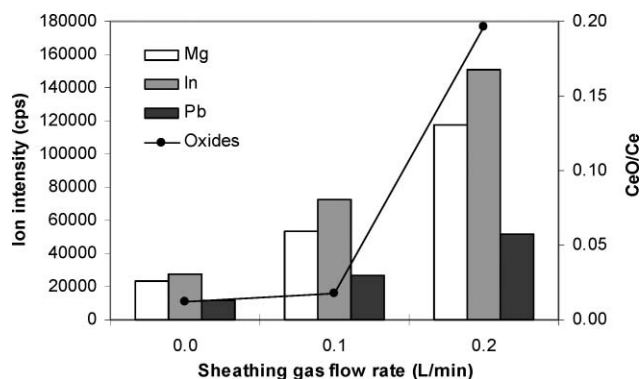


Fig. 2 Effect of sheathing gas flow rate on sensitivity and oxides formation.

improved by a factor of about 6, whereas for CeO/Ce this increase factor was close to 10. This fact clearly suggested deterioration in the plasma thermal characteristics. Note that in absence of plasma effects both ratios would be the same. In order to obtain maximum sensitivity while limiting oxides formation, this parameter was set at 0.1 l min^{-1} . Under this condition, the signal was about twice than in absence of sheathing gas and the $^{156}\text{CeO}^+ / ^{140}\text{Ce}^+$ ratio was lower than 2%. The effect of the nebulizer gas flow rate on sensitivity and oxides formation is shown in Fig. 3, with the trend obtained for $^{115}\text{In}^+$ representing the general behaviour. It can be seen that the ion intensity peaked at 0.9 l min^{-1} . On the other hand, under this condition the oxides ratio was quite high and a compromise value of 0.8 l min^{-1} was selected as the optimal one. Finally, the sample uptake rate was set at $20 \mu\text{l min}^{-1}$, although higher values (at least up to $80 \mu\text{l min}^{-1}$) could be used without observing any liquid condensation on the chamber walls. However, the application of a low sample consumption rate allowed the analytical program (determination of nine analytes, under three DRC conditions, see Table 2) to be carried out, while consuming less than $200 \mu\text{l}$ of sample.

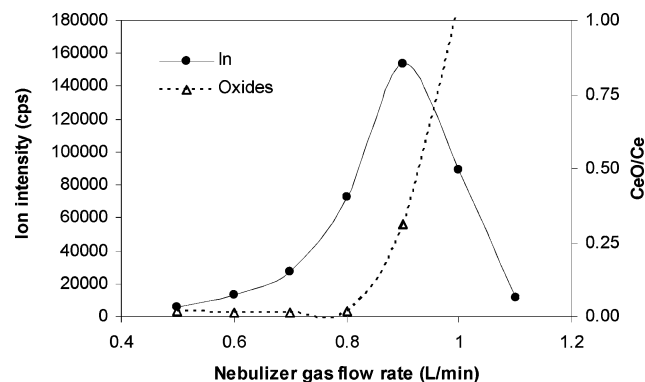


Fig. 3 Effect of nebulizer gas flow rate on sensitivity and oxides formation.

The performance characteristics of the optimized sample introduction system were evaluated for a number of analytes and compared with those obtained using a conventional microsample introduction system, consisting of the PFA micronebulizer (the same as that used for TISIS) coupled to a low inner volume cyclonic spray chamber (Cinnabar). The results are reported in Table 3. It can be seen that TISIS compares favourably with respect to the Cinnabar in terms of sensitivities and limits of detection. The result can be ascribed to the combined effect of the increased chamber temperature and of the sheathing gas stream, which enhanced aerosol evaporation and transport towards the ionization source. Moreover, in the case of TISIS, the path towards the plasma is very easy, hence making the analyte impact losses to be less intense than for the Cinnabar.

Optimization of the DRC conditions

Although snow represents a quite “clean” matrix, polyatomic interferences may occur and affect the analytical accuracy of the ICP-MS analysis, due to the very low concentration levels at which the considered analytes usually occur in snow samples from remote areas. The solvent (0.05% nitric acid solution) causes the formation of $^{36}\text{Ar}^{14}\text{NH}^+$, $^{40}\text{Ar}^{14}\text{NH}^+$ and

Table 3 Comparison of performance characteristics for the TISIS and a conventional micro-sample-introduction system (PFA micronebulizer + Cinnabar cyclonic spray chamber)

Analyte	Sensitivity ^a (counts s ⁻¹ ng ⁻¹ ml)		Limit of detection ^b (pg ml ⁻¹)	
	TISIS	PFA + Cinnabar	TISIS	PFA + Cinnabar
Cr	6159	2869	1.5	8.3
V	2124	1664	4.4	4.6
Fe	12 283	3947	3.6	11.0
Mn	13 044	6094	4.1	8.9
Pb	16 732	9434	0.8	5.9
Zn	2258	1683	37	77
Cd	6744	4106	1.9	4.9
Co	12 999	5529	1.6	4.1
Cu	6845	3155	5.0	9.9

^a Slope of the calibration curve ($r > 0.9999$); ^b 3σ criterion, $n = 20$. Sample uptake rate: 20 $\mu\text{l min}^{-1}$.

⁴⁰Ar¹⁶O⁺ ions, which overlap ⁵¹V⁺, ⁵⁵Mn⁺ and ⁵⁶Fe⁺, respectively, when using a quadrupole ICP-MS. Moreover, after the pre-concentration step, the sample may contain small amounts of Na, Ca and Cl, giving rise to the formation of ³⁵Cl¹⁶OH⁺, ³⁵Cl¹⁶O⁺, ³⁷Cl¹⁴N⁺, ⁴⁰Ca¹⁶O⁺ and ⁴⁰Ar²³Na⁺ species, which may further affect the determination of ⁵¹V⁺, ⁵²Cr⁺, ⁵⁶Fe⁺ and ⁶³Cu⁺ isotopes. In order to resolve these polyatomic interferences, the dynamic reaction cell technique^{27–29} was applied. The optimization of the relevant operating parameters (mainly, the reactive gas flow rate and the Mathieu stability parameters of the cell's quadrupole) was performed according to Tanner *et al.*²⁹ An example of the reaction profile is shown in Fig. 4. It was obtained by plotting the ion intensity at $m/z = 56$ (in logarithmic scale) against the reactive gas flow rate for a blank solution (0.05% nitric acid) and a sample solution (100 ng l⁻¹ iron standard solution). The initial decay reflects the rate of loss of the interfering species (⁴⁰Ar¹⁶O⁺), due to the reaction with the reactive gas (ammonia). When the transmitted ion signal is dominated by the analyte ion (⁵⁶Fe⁺), a further linear decay was observed, corresponding to the slower rate of reaction/scattering of the analyte ion. By selecting a reaction gas flow rate of 1.0 ml min⁻¹, the polyatomic interference can be reduced by three orders of magnitude, obtaining a satisfactory signal-to-background ratio. Analogous optimization experiments led to the DRC conditions summarized in Table 2. Interestingly, for Cu, Co and Zn, the use

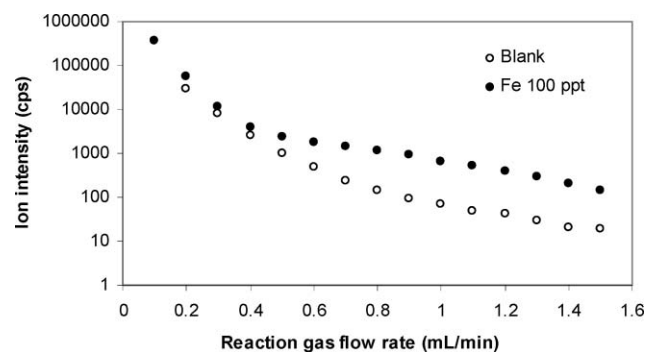


Fig. 4 Ion intensity at $m/z = 56$ as a function of the ammonia flow rate. ○ blank (0.05% nitric acid solution); ● sample (100 ng l⁻¹ Fe standard solution).

Table 4 Analysis of the 100-fold diluted certified reference water TM-23.3 (values in ng l⁻¹)

Analyte	Found	Certified
Cr	64 ± 6	66 ± 5
V	17 ± 2	21 ± 2
Fe	148 ± 7	150 ± 33
Mn	86 ± 3	87 ± 4
Pb	33 ± 1	32 ± 3
Cd	25 ± 1	25 ± 2
Co	75 ± 2	67 ± 5
Cu	94 ± 3	91 ± 6

of the DRC was found to be unnecessary, possibly because of the very low concentration of the concomitant elements. Hence, any multi-elemental analysis consisted of three steps, carried out sequentially. Since switching from one DRC condition to another is quite fast and the sample consumption rate very low, this analytical program could be performed in a period of time as short as 6 min (including sample delivering and washing times), while consuming less than 200 μl of sample.

Development of the pre-concentration procedure

In spite of the excellent detection limits achieved by the optimized ICP-MS system (Table 3), these were not sufficiently low for direct determination of trace elements in the snow of remote polar regions. Therefore, a pre-concentration procedure was developed. It has been claimed that pre-concentration can be a source of contamination. For this reason the method applied in the present work, simply consisted of a solvent removal step by freeze-drying, followed by re-dissolution with 200 μl of 0.05% nitric acid. Freeze-drying was preferred to sub-boiling evaporation, due to the following advantages: (i) the procedure can be applied directly to frozen samples; (ii) the process can be carried out until dryness, making the calculation of the pre-concentration factor easier; (iii) the sample preparation can be performed overnight, without any need to control it; (iv) the procedure can be accomplished in a closed environment, thus reducing the risk of contamination. The accuracy of the pre-concentration procedure was verified by using the certified reference water TM-23.3, supplied by Environmental Canada's NWRI (web site in the experimental section). In order to match the certified analytical concentrations with the real ones, the standard was 100-fold diluted. The resulting concentrations ranged from 20 to 150 ng l⁻¹. Then, 20 ml aliquots were freeze-dried, re-dissolved in 200 μl of 0.05% nitric acid solution and analysed by ICP-MS, under the conditions previously optimized. The results are reported in Table 4. It was deduced that the pre-concentration procedure is accurate (t -test, 95% confidence level) and precise (RSD% < 6%, $n = 4$). The procedure was tested at different pre-concentration ratios, from 1 : 10 to 1 : 100. For example, the ⁵⁶Fe⁺ ion intensity as a function of the initial sample volume for the CRM and one real sample collected in the remote site of Dome C (Antarctica) are plotted in Fig. 5.

Analytical figures

The optimized analytical procedure was applied both to filtered (0.5 μm) and unfiltered acidified (0.5% nitric acid) snow

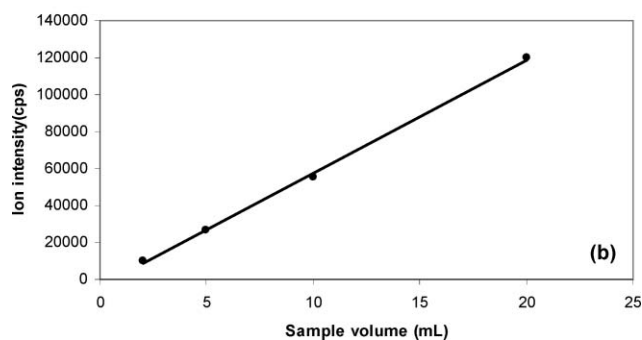
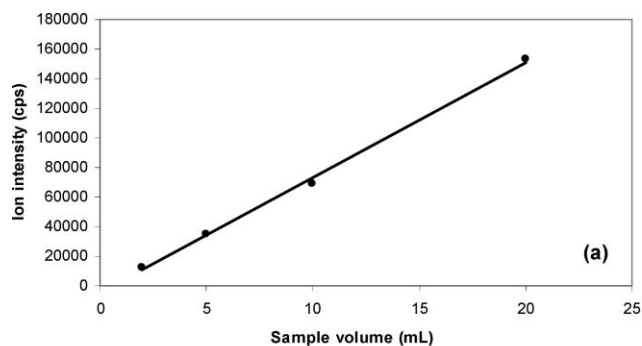


Fig. 5 $^{56}\text{Fe}^+$ ion intensity as a function of the sample volume. (a) Certified water TM-23.3 (diluted 1.100). (b) Surface snow sample (Dome C, Antarctica).

samples. In the former case, dissolved element concentrations are obtained, while in the second case—corresponding to the usually reported treatment of snow and ice samples (e.g. ref. 8,20)—the acid dissolvable element concentrations are obtained. The detection limits of these procedures, calculated as three times the standard deviation of ten procedural blanks, are reported in Table 5. The ranges of LOD-values reported for the direct analysis of Antarctic snow samples using high resolution ICP-MS are also reported for comparison. It can be seen that the achieved detection limits are extremely low, making the developed method suitable for the analytical task. As stated above, the accuracy and precision of the method was verified using the certified reference water TM-23.3 (Table 4). The found values were not significantly different from the certified ones. Precision of the procedure ranged from 2.0% to 5.6%.

Application to real samples

Finally, the developed procedure was applied to a number of surface snow samples collected in three Antarctic sites, in the framework of the Italian National Antarctic Research Programme (PNRA). Data are summarized in Table 6. Instrumental precision of each determination was always lower than 10% (often lower than 5%) and the found concentrations were significantly higher than the limits of detection of the procedure (Table 5). Element concentrations detected in snow samples collected in the pristine sites of Dome C and Talos Dome are in good agreement with values reported by other authors.^{8,20,21} As expected, the acid dissolvable element concentrations were higher than the dissolved element ones, due to the contribution

Table 5 Limits of detection of the procedure (values in pg g^{-1})^a

Analyte	LOD for dissolved element determination	LOD for acid dissolvable element determination	LOD using high resolution ICP-MS ^b
Cr	0.04	0.05	0.2–0.25
V	0.07	0.09	0.49–2
Fe	0.37	0.59	4.2–48
Mn	0.18	0.22	0.2–2
Pb	0.04	0.53	0.09–0.5
Zn	2.30	4.53	0.9–7.26
Cd	0.02	0.04	0.3–1.96
Co	0.03	0.03	0.09–2
Cu	0.17	1.46	0.52–0.8

^a Based on the standard deviation of the ten procedural blanks. Pre-concentration factor: 100. ^b Data from ref. 8, 20–22.

Table 6 Dissolved (D) and acid dissolvable (AD) element concentration ranges in Antarctic snow samples (values in pg g^{-1})

Analyte	Inland ^a		Coastal ^b	
	D ($n = 8$)	AD ($n = 4$)	D ($n = 9$)	AD ($n = 8$)
Cr	1.4–6.5	3.8–11	0.7–10	2.7–67
V	1.0–2.1	0.5–2.1	1.6–19	4.0–10
Fe	18–84	30–467	34–272	501–2807
Mn	4.4–18	10–28	30–350	52–151
Pb	1.7–24	5.6–14	0.7–43	3.8–51
Zn	85–320	431–678	215–527	126–1692
Cd	0.5–4.2	1.5–2.7	0.6–14	0.8–29
Co	0.2–0.9	0.3–1.3	0.9–10	1.9–17
Cu	10–46	6.6–43	15–114	19–442

^a Terra Nova Bay ($74^\circ 43' \text{N}$; $164^\circ 0' 7' \text{E}$). ^b Talos Dome ($72^\circ 50' \text{S}$ $159^\circ 12' \text{E}$; elevation: 2300 m; 275 km from the coast) and Dome C ($75^\circ 0' 7' \text{N}$; $123^\circ 19' \text{E}$; elevation: 3200 m; 1200 km from the coast).

of the particulate matter, and the concentration values found for the coastal site of Terra Nova Bay were higher than those observed for the samples collected on the Antarctic plateau.

Conclusions

This work showed that by combining a simple pre-concentration procedure with the application of the ICP-DRC-MS technique, it is possible to accurately determine various trace metals at extremely low concentration levels. This task was achieved by the optimization of the DRC conditions for reducing the polyatomic interferences and the use of a new total-consumption micro-sample-introduction system, capable of introducing small volumes of pre-concentrates at a very low consumption rate with high sensitivity and precision. The analysis of both certified and real samples showed the suitability of the proposed method for the analysis of polar snow samples.

References

- 1 C. F. Boutron, *Environ. Rev.*, 1995, **3**, 1–28.
- 2 C. F. Boutron, J. P. Vandelone and S. Hong, *Geochim. Cosmochim. Acta*, 1995, **58**, 3217–3225.
- 3 C. Barbante, G. Cozzi, G. Capodaglio, K. Van, de Velde, C. Ferrari, A. Veysseyre, C. F. Boutron, G. Scarponi and P. Cescon, *Anal. Chem.*, 1999, **71**, 4125–4133.

-
- 4 F. A. M. Planchon, C. F. Boutron, C. Barbante, G. Cozzi, V. Gasparic, E. W. Wolff, C. P. Ferrari and P. Cescon, *Earth Planet. Sci. Lett.*, 2002, **200**, 207–222.
 - 5 E. D. Suttie and E. W. Wolff, *Atmos. Environ., Part A*, 1993, **27**, 1833–1841.
 - 6 C. F. Boutron and C. C. Patterson, *J. Geophys. Res., [Atmos.]*, 1987, **92**, 8454–8464.
 - 7 S. D. Hur, X. Cunde, S. Hong, C. Barbante, P. Gabrielli, K. Lee, C. F. Boutron and Y. Ming, *Atmos. Environ.*, 2007, **41**, 8567–8578.
 - 8 F. A. M. Planchon, C. F. Boutron, C. Barbante, E. W. Wolff, G. Cozzi, V. Gasparic, C. P. Ferrari and P. Cescon, *Anal. Chim. Acta*, 2001, **450**, 193–205.
 - 9 E. W. Wolff, M. P. Landy and D. A. Peel, *Anal. Chem.*, 1981, **53**, 1566–1570.
 - 10 U. Görlach and C. F. Boutron, *Anal. Chim. Acta*, 1990, **236**, 391–398.
 - 11 E. D. Suttie and E. W. Wolff, *Anal. Chim. Acta*, 1992, **258**, 229–236.
 - 12 M. A. Bolshov, C. F. Boutron, F. M. Ducroz, U. Görlach, O. N. Kompanetz, S. N. Rudniev and B. Hutch, *Anal. Chim. Acta*, 1991, **251**, 169–175.
 - 13 M. A. Bolshov, S. N. Rudnev, J. P. Candelone, C. F. Boutron and S. Hong, *Spectrochim. Acta, Part B*, 1994, **49**, 1445–1452.
 - 14 M. A. Bolshov, S. N. Rudnev, A. A. Rudnieva, C. F. Boutron and S. Hong, *Spectrochim. Acta, Part B*, 1997, **52**, 1535–1544.
 - 15 J. Völkening and K. G. Heumann, *Fresenius' J. Anal. Chem.*, 1988, **331**, 174–181.
 - 16 G. Scarponi, C. Barbante, C. Turetta, A. Gambero and P. Cescon, *Microchem. J.*, 1997, **55**, 24–32.
 - 17 M. Koyama, J. Takada, K. Kamiyama, N. Fujii, J. Inoue, K. Issiki and E. Nakayama, *J. Radioanal. Nucl. Chem.*, 1988, **124**, 235–249.
 - 18 T. D. Jickells, T. D. Davies, M. Tranter, S. Landsberger, K. Jarvis and P. Abrahams, *Atmos. Environ., Part A*, 1992, **26**, 393–401.
 - 19 R. E. Sturgeon, S. N. Willie, J. Zheng, A. Kudo and D. C. Grégoire, *J. Anal. At. Spectrom.*, 1993, **8**, 1053–1058.
 - 20 C. Barbante, T. Bellomi, G. Mezzadri, P. Cescon, G. Scarponi, C. Morel, S. Jay, K. van de Velde, C. P. Ferrari and C. F. Boutron, *J. Anal. At. Spectrom.*, 1997, **12**, 925–931.
 - 21 A. T. Townsend and R. Edwards, *J. Anal. At. Spectrom.*, 1998, **13**, 463–468.
 - 22 M. Bensimon, J. Bourquin and A. Parriaux, *J. Anal. At. Spectrom.*, 2000, **15**, 731–734.
 - 23 N. M. Reed, R. O. Cairns, R. C. Hutton and Y. Takaku, *J. Anal. At. Spectrom.*, 1994, **9**, 881–896.
 - 24 C. Barbante, G. Cozzi, G. Capodaglio, K. Van, de Velde, C. Ferrary, C. Boutron and P. Cescon, *J. Anal. At. Spectrom.*, 1999, **14**, 1433–1438.
 - 25 J. L. Todolí and J. M. Mermet, *J. Anal. At. Spectrom.*, 2002, **17**, 345–351.
 - 26 C. Lagomarsino, M. Grotti, J. L. Todolí and J. M. Mermet, *J. Anal. At. Spectrom.*, 2007, **22**, 523–531.
 - 27 V. I. Baranov and S. D. Tanner, *J. Anal. At. Spectrom.*, 1999, **14**, 1133–1142.
 - 28 S. D. Tanner and V. I. Baranov, *J. Am. Soc. Mass Spectrom.*, 1999, **10**, 1083–1094.
 - 29 S. D. Tanner, V. I. Baranov and U. Vollkopf, *J. Anal. At. Spectrom.*, 2000, **15**, 1261–1269.
 - 30 F. Soggia, M. L. Abemoschi, S. Dalla, Riva, R. De, Pellegrini and R. Frache, *Int. J. Environ. Anal. Chem.*, 2000, **79**, 367–378.
 - 31 W. C. Wetzel, J. A. C. Broekaert and G. M. Hieftje, *J. Anal. At. Spectrom.*, 2005, **20**, 621–625.
 - 32 M. A. Tarr, G. Zhu and R. F. Browner, *J. Anal. At. Spectrom.*, 1992, **7**, 813–817.
 - 33 M. P. Field and R. M. Sherrell, *J. Anal. At. Spectrom.*, 2003, **18**, 254–259.